COMPLEX FLUID MIXING IN MICRO-FLUIDIC DEVICES: THEORY AND SIMULATIONS

Srikanth DHONDI[1] and <u>Gerald G. PEREIRA</u>[2*]

[1] School of Chemical and Physical Sciences, Victoria University, Wellington, NEW ZEALAND

[2] CSIRO Mathematical & Information Sciences, Clayton, Victoria 3169, AUSTRALIA
*Corresponding author, E-mail address: Gerald.Pereira@csiro.au

ABSTRACT

Micro and nano-fluidic mixing is now an important area of scientific research because of its applications in significant areas such as electrophoresis systems, chemical and bio-chemical synthesis. Fluid flow at these small dimensions is necessarily laminar and, as such, dominated by diffusion which is extremely slow. Furthermore, more realistic applications deal with viscoelastic fluids where it is well known dynamics are significantly slower than for simple fluids. In this study we consider how mixing can be enhanced by using some clever techniques such as chemical patterning of the micro-fluidic tube walls for non-Newtonian and viscoelastic fluids. We use both continuum modelling and molecular dynamics simulations to describe these slow flows and outline some important ways in which fluid mixing can be promoted in these devices.

NOMENCLATURE

L characteristic length
p pressure
$\mathbf{u}$ velocity field
ρ fluid density

INTRODUCTION

Micro and nano-fluidics is a rapidly growing area of fluid mechanics with potential applications in chemical, biomedical and biochemical processes (Nguyen and Wu, 2005, Ottino and Wiggins, 2004). In general, one deals with small amounts of reagents and rapid mixing of fluids is vital to efficiency of the process. However, when one gets down to the micro and nano length scales, it is well known that fluid flow becomes laminar and thus mixing is diffusion dominated. This is an extremely slow process and hence the future of this field depends on developing new and novel techniques to enhance fluid mixing.

Most of the fluids one deals with in practice are not described by simple (Newtonian) fluid models. In general, most applications deal with so called "*complex fluids*" which are usually polymeric in nature. In this case, it is well known that fluid flow (and hence mixing) is slowed down even further due to the complex motion of these molecules (Doi and Edwards, 1999, Bird *et al.* 1987). In this study we therefore consider techniques to enhance mixing for complex fluids which have both a non-Newtonian viscosity behaviour and an elastic response, hence the name viscoelastic fluids.

In this study we will implement a continuum fluid mechanics model and consider a couple of methods to enhance mixing in narrow channels. The first method we

use is to use chemically patterned boundary conditions with alternating regions of high and low slip. Hendy (2005) has shown these boundary conditions can induce transverse flows in Newtonian fluids and thus we question if similar flows are induced for viscoelastic fluids. Since these fluids are also elastic in nature we propose, in addition, to use an oscillating pressure gradient to drive the fluid along the channel. The continuum model is valid as long as the width of the channel is large in comparison to molecule size, however when one gets down to small length scales, it is not clear when this model breaks down. To answer this question and also validate the continuum theory predictions we therefore carry out particle based simulations, which bypass any assumptions of the continuum theory.

CONTINUUM THEORY

We outline the continuum theory which is used to model flow of inelastic fluid in a channel. For simplicity, we restrict ourselves to two-dimensions so that we effectively have flow between plates. The channel is aligned so that its axis runs along the *x*-axis and is of length L and width $2w$ (in the *y*-direction). Thus the fluid flows in the region $-w < y < w$ and $0 \leq y \leq L$. A pressure difference, Δp, is applied along the length of the channel so that $p(x) = p_0 - \Delta p x / L$. The Navier-Stokes equations for an incompressible fluid in the absence of gravity is

$$\nabla \cdot \mathbf{u} = 0 \quad , \qquad (1)$$

$$\rho \left(\frac{\partial \mathbf{u}}{\partial t} + \mathbf{u}\nabla \cdot \mathbf{u} \right) = -\nabla \cdot \underline{\underline{\Pi}} \quad , \quad (2)$$

where $\underline{\underline{\Pi}} = p\underline{\underline{I}} + \underline{\underline{\tau}}$, $\mathbf{u}$ is the velocity field given by $[u,v,0]$, ρ is the fluid density, $\underline{\underline{\tau}}$ is the stress tensor and $\underline{\underline{I}}$ is the unit tensor. Since we are dealing with non-Newtonian fluids we specify the relationship between stress and strain-rate. We use the Ostwald-de Waele power-law model (Bird, 1987)

$$\underline{\underline{\tau}} = -\eta(\dot{\gamma})\underline{\underline{\dot{\gamma}}} ; \dot{\gamma} = \left[\frac{1}{2} Tr\left(\underline{\underline{\dot{\gamma}}} \cdot \underline{\underline{\dot{\gamma}}} \right) \right]^{1/2} ; \eta(\dot{\gamma}) = m(\dot{\gamma})^{n-1},$$

$$(3)$$

where $\underline{\underline{\dot{\gamma}}}$ is the rate-of-strain tensor and $\dot{\gamma}$ is related to the second invariant of the rate-of-strain tensor. In Eq.(3) the exponent n defines the nature of the fluid. For $n<1$ we have a shear-thinning fluid (which corresponds to most macromolecular type fluids) while for $n>1$ we have a

shear-thickening fluid (which usually involves some kind of molecular network). To solve these two equations we impose slip boundary conditions at $y = \pm w$. The slip boundary condition is $u(\pm w) = \delta(\partial u / \partial y)_{y=\pm w}$ where δ is the slip length (Hendy *et al*, 2005). If there is no variation in the boundary condition in the x direction then the steady-state, laminar flow solution is straightforward (and Pouseille-like), i.e.,

$$u(y) = \left(\frac{\Delta p}{L}\frac{w}{m}\right)^{1/n}\left[\frac{w}{1+1/n}\left\{1-\left(\frac{y}{w}\right)^{1+1/n}\right\}+\delta\right],$$

(4)

which is valid for $y \geq 0$ (for negative y, $y \to -y$). The flow is purely in the axial direction. To obtain mixing (due to fluid flow) we need to induce transverse flow into the channel. As discussed above, this is done by using patterned boundary conditions (alternating regions of high and low slip). Thus we model this by a sinusoidal variation in the slip boundary condition (with wave-number, k and small amplitude α) i.e.

$$u(x, y = w) = -\delta(1+\alpha e^{ikx})\left(\frac{\partial u}{\partial y}\right)_{y=w}. \qquad (5)$$

With a variation in the slip boundary conditions, one would expect the fluid flow would involve both longitudinal and transverse flow. In addition each of these components would be a function of both x and y. In Eq. (5), α is assumed to be small so that a perturbation expansion is valid,

$$u = u_0 + \alpha u_1 + O(\alpha^2)$$
$$v = \alpha v_1 + \ldots$$
$$p = p_0 - \Delta\left(\frac{x}{L}\right) + \alpha p_1 + \ldots \qquad (6)$$
$$\underline{\underline{\tau}} = \underline{\underline{\tau}}^0 + \alpha\underline{\underline{\tau}}^1 + \ldots$$

Note that u_0 is given by Eq. (4) so that we now need to solve at $O(\alpha)$ which requires some algebra. Doing this one can show u_1 and v_1 are separable and of the form

$$u_1(x,y) = e^{ikx}f'(y) \quad v_1(x,y) = -ike^{ikx}f(y), \quad (7)$$

where the prime denotes a derivative with respect to y. The presence of an imaginary number in the solution for v_1 indicates this velocity is out of phase with u_1. Completing the necessary algebra one finds f satisfies a fourth-order linear ordinary differential equation:

$$y^2\frac{d^2f}{dy^2} + 2\aleph y\frac{d^3f}{dy^3} + \left[2y^2k^2\Re - \aleph/n\right]\frac{d^2f}{dy^2} +$$

(8)

$$2\aleph\Re k^2y\frac{df}{dy} + k^2\left[k^2y^2 - \aleph/n\right]f = 0,$$

where $\aleph \equiv 1-1/n$ and $\Re \equiv 1-2/n$. There are correspondingly four boundary conditions:

$f(0) = f(w) = f''(0) = 0$ and

$f'(w) + \delta f''(w) = \delta U^{1/n}$ where $U \equiv \Delta pw/Lm$.

Numerical solutions for a variety of n values are shown in Fig. 1 and indicate that larger transverse velocities are generated for shear-thickening fluids in comparison to a Newtonian fluid, while the shear-thinning fluids have the smallest transverse velocity. We also find the largest transverse velocities are generated for values of $kw=3$, i.e., the length of a patterned region should be roughly similar to the channel width.
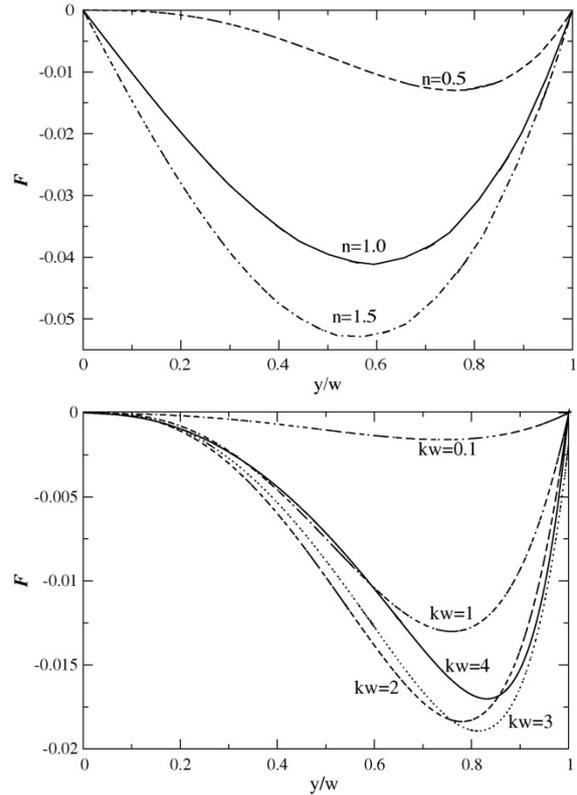
Figure 1: Function $F \equiv kf/wU^{1/n}$ as a function of y/w for various n obtained by solving Eq. (8) (top) and $n=0.5$ but various values of kw (bottom).

Time varying pressure head

We have seen that the transverse flows can be generated by using a variation in the boundary conditions. However, we would like to increase the magnitude of these velocities, especially for shear thinning fluids. We suggest this can be done by using the elastic property of the complex fluids. The idea here is that by imposing a sinusoidal pressure gradient the magnitude of the fluid flow velocity will increase due to a resonance-like effect. We use the same theory as has just been described but now the imposed pressure head is given by

$$p = p_0 - \Delta p\left(\frac{x}{L}\right)\left(1 + \varepsilon e^{i\omega t}\right) \qquad (9)$$

where ε is a small parameter and ω is the frequency of the sinusoidal oscillation. We now need to supply a suitable constitutive equation for the visco-elastic fluid and we use a relatively simple linear model which will demonstrate the general strategy behind this idea. The constitutive model we use is the linearized White-Metzner

model, with a power law viscosity function (Tanner, 2002, Barnes *et al*, 1989):

$$\underline{\underline{\tau}} + \lambda \frac{\partial \underline{\underline{\tau}}}{\partial t} = -\eta(\dot{\gamma})\underline{\underline{\dot{\gamma}}}, \qquad (10)$$

where λ is a typical "relaxation time" for the polymeric fluid. We follow the same procedure as before, except now we make a perturbation expansion for α and ε. In addition to the terms given in Eq. (6), there are now order ε terms. However, these terms will not contribute to the transverse flow (only flow in the axial direction). Hence to obtain the next correction to the transverse flow we need to consider order $\alpha\varepsilon$ terms which are time dependent. One can show the important corrections for longitudinal and transverse flow are then

$$u_{\alpha\varepsilon} = \alpha\varepsilon e^{i(kx+\omega t)}g'(y)$$
$$v_{\alpha\varepsilon} = -ik\alpha\varepsilon e^{(ikx+wt)}g(y) \qquad (13)$$

and *g(y)* is given by $g(y) \equiv n^{-1}\exp(i\phi)\left(1+\lambda^2\omega^2\right)^{1/2}\zeta(y)$ and $\phi \equiv \tan^{-1}(\lambda\omega)$. In this solution for g, ζ is given by the solution of the fourth order linear differential equation:

$$y^2 \frac{d^2\zeta}{dy^2} + 2\aleph y\frac{d^3\zeta}{dy^3} + \left[2y^2k^2\Re - \aleph/n\right]\frac{d^2\zeta}{dy^2} + \qquad (12)$$

$$2\aleph\Re k^2 y\frac{d\zeta}{dy} + k^2\left[k^2y^2 - \aleph/n\right]\zeta = \xi(y),$$

where

$$\xi(y) = 2\aleph \begin{bmatrix} (3/n-1)(1+1/n)(f''+k^2f) \\ +2k^2\left(\frac{y^2}{n}\frac{d^2f}{dy^2}+y\aleph\frac{df}{dy}\right) \end{bmatrix} \qquad (13)$$

and the boundary conditions for ζ are the same as the boundary conditions for *f*. The most important thing to note about the solution for *g* is that it involves the multiplicative factor $\left(1+\lambda^2\omega^2\right)^{1/2}$. Recall λ depends on the particular material being considered and so cannot be controlled but the driving frequency can be changed. Thus by increasing ω we can effectively increase the magnitude of the transverse velocity. All we require to do now is to make sure that ζ is of similar order in magnitude to *f*. Once again we can solve for ζ numerically and Fig. 2 shows the solution for various shear thinning cases. It is quite clear that ζ is of similar order to *f*.

Summary of continuum predictions

The continuum model has shown that the basic flow of a non-Newtonian viscous fluid in a narrow channel, subject to variable slip boundary conditions, results in flows

$$\mathbf{u} = \hat{\mathbf{i}}\left[u_0(y) + \alpha e^{ikx}f'(y)\right] + \hat{\mathbf{j}}\alpha e^{i(kx-\pi/2)}f(y). \qquad (14)$$

Mixing will be beneficial (compared to a Newtonian fluid) for shear-thickening fluids but will be suppressed for shear-thinning fluids. To understand the flow patterns created by these patterned boundaries we present a schematic of the streamlines for the velocity profile in Fig. 3. (Note, the u_0 term is not included, as this is constant along the channel length.) The points of zero flow are

given by $x = ... - 2\pi/k, -\pi/k, 0, \pi/k, 2\pi/k...$ and $y = y_0$ where y_0 satisfies $f'(y_0) = 0$. All flows circulate about these points either in the clockwise or anti-
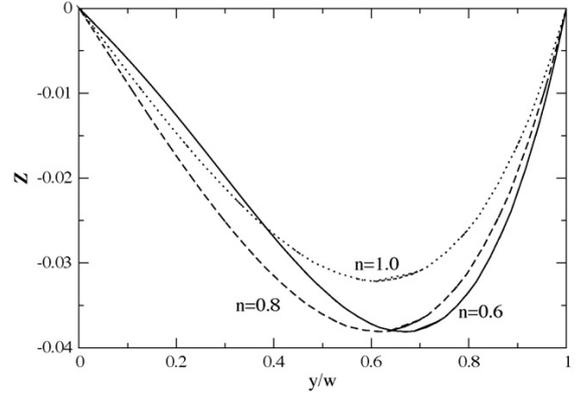
Figure 2: Function $Z \equiv k\zeta/wU^{1/n}$ for various *n* obtained by solving Eqs. (12) and (13).

clockwise sense depending on whether $\delta(x)$ is greater or less than the average slip length. At *x* values such that $x = ... - 3\pi/2k, -\pi/2k, \pi/2k, 3\pi/2k...$ the axial component of the velocity is zero so that at these values of *x* there is only a transverse component. To induce larger transverse flows for shear-thinning fluids we suggest the elastic property of these fluids can be exploited to increase the transverse flow. This can be done by applying a sinusoidal time varying pressure profile.
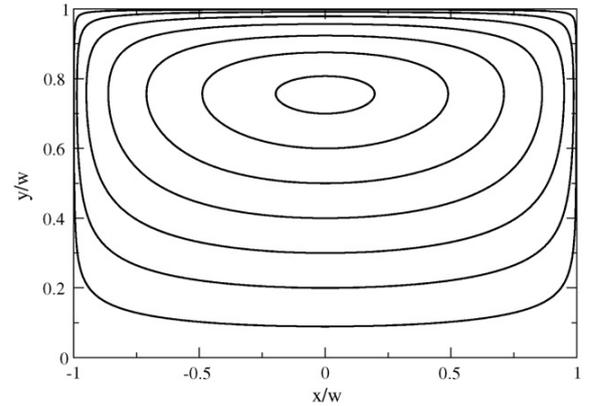
Figure 3: Schematic of streamlines at $O(\alpha)$ velocity flow for the Ostwalde de Waale model (for *n*=0.5). The flow circulates in a clockwise manner around the zero flow point at *x*=0 and *y/w*=0.76, which is the solution of $f'(y) = 0$. In the adjacent regions -3<*x/w*<-1 and 1<*x/w*<3 the streamline pattern is the same except the flow is anti-clockwise about the zero flow point. This streamline pattern is replicated along the entire channel length.

MOLECULAR MODEL

So far we have given theoretical predictions based on a continuum model of the polymeric fluid. We would like to now implement a completely independent validation of these predictions. In the absence of experiments, the next best method to validate these predictions is first principle computer simulation. Here we input the important molecular interactions into the problem and then let the

3

system evolve naturally. The computer simulation method we use is molecular dynamics (MD) and this method is implemented for two main reasons. Firstly, the MD method is a particle-based method and hence does not make any assumptions regarding the continuum nature of the problem. Since we are dealing with small dimensions, this is an important consideration and our MD results will show that in fact the continuum assumptions are indeed valid. Secondly, the MD method is appropriate because by simulating at a particle level we will gain extra insights into the problem which are not addressed in the continuum model.

The MD method we use is well known and we will not go too much into the details of the technique. The interested reader is referred to relevant literature (Allen and Tildesley, 1987). We mention here only the important points for our study. The essentials of the technique (for us) are as follows. For each particle we solve Newton's equation of motion where the force is due to the spatial gradient of the intermolecular potential and any externally applied force. Recall, we are dealing with polymeric molecules which are modelled as bonded chains. Bonds (between adjacent monomers) are modelled by a finite extensible nonlinear elastic (FENE) potential - essentially a Hookean spring for small extension and for large extension a much larger restoring force (Grest and Kremer, 1986). Each polymeric chain is made up of 20 monomers. There is also a Lennard-Jones potential between any monomers and between wall atoms and monomers. It is of the form

$$\Phi_{LJ}(r) = \kappa\left[\left(\frac{\sigma}{r}\right)^{12} - \left(\frac{\sigma}{r}\right)^{6}\right], \qquad (15)$$

where r is the separation between any two particles and κ and σ are the energy and length scales in the simulation. The first term in the square brackets prevents particles overlapping in space while the second term represents an attraction between particles. κ varies according to the type of particles that are involved in the binary interaction and is tuned for the particular pair of particles being considered. It is the important parameter in setting the boundary (slip) conditions. The channel is set-up in the same way as outlined in the "Continuum theory" section with the only change being that we implement periodic boundary conditions in the x and z directions. This is required since as we are modelling at the particle scale we cannot simulate too many stripes (which would require an enormous number of particles and hence enormous computational times). The equations of motion were integrated using the Verlet algorithm (Allen and Tildesley, 1987). Polymeric chains completely fill the domain to a monomer number density of $0.9\sigma^{-3}$.

Fluid characterisation

The first thing we need to do is fully characterize our polymeric fluid and relate it to the continuum theory. To do this we first ran a set of Couette simulations. This involves moving one of the walls at a prescribed velocity, V, and then calculating the resulting shear stress in the fluid. The fluid viscosity is then given by

$$\eta = \tau_{xy}\big/\dot{\gamma} \qquad \text{where} \qquad \dot{\gamma} = V\big/2w \qquad (16)$$

and the shear stress is calculated according to standard methods (Jabbarzadeh et al, 2003). Doing this for a number for a number of different shear rates, we determined our polymeric fluid to be have an n value of 0.6076 ± 0.0138. Thus we have a shear-thinning fluid. By doing a set of Pouseille simulations (homogenous boundary conditions) we were then able to determine the relationship between κ (between wall atoms and monomers) and the slip length, δ.
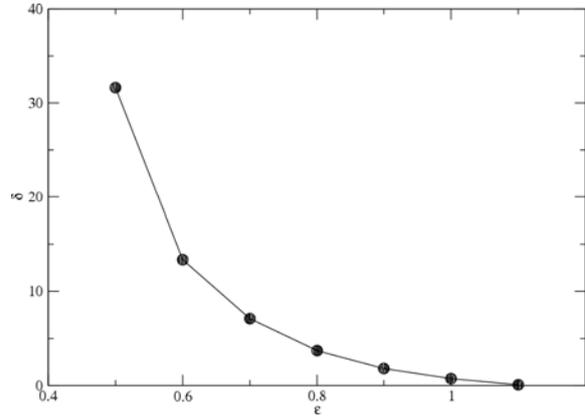
Figure 4: Slip length, δ as a function of interaction energy parameter between wall atoms and monomers from the molecular dynamics simulations. The dots represent values of interaction parameter which were simulated.

Figure 4 shows the results for these simulations and indicates that as we increase the magnitude of the interaction between the wall atoms and monomers the slip length correspondingly decreases. Intuitively, this makes sense since by increasing this interaction monomers are attracted more strongly by the walls atoms and hence tend to stick to these atoms. Hence the flow velocity of these monomers must decrease and hence the slip length correspondingly decreases. In the remainder of the simulations where we pattern the walls we will use two different values of the wall-monomer interaction and create regions of different slip. In contrast to the theoretical pattern which had a sinusoidal profile, the pattern in the MD simulations has a square wave profile. However, as long as the difference in slip length between the two patterned regions is relatively small previous work on Newtonian fluids (Hendy et al, 2005) has shown that the square-wave profile gives similar flows to a sinusoidal patterned profile.

Patterned boundaries (constant pressure)

We now proceed to reporting on simulations where we used the patterned boundary conditions. Recall the main aim here is to determine whether these patterned boundary conditions can induce significant transverse flows. A constant pressure gradient is applied between the channel ends (and this is done in the MD simulation by applying a constant external force in the positive x-direction on each monomer). The patterned regions we used corresponded to interaction parameters between wall atoms and monomers of 0.9 and 0.5 (see Fig. 4 for corresponding slip-length).

4

t = 531
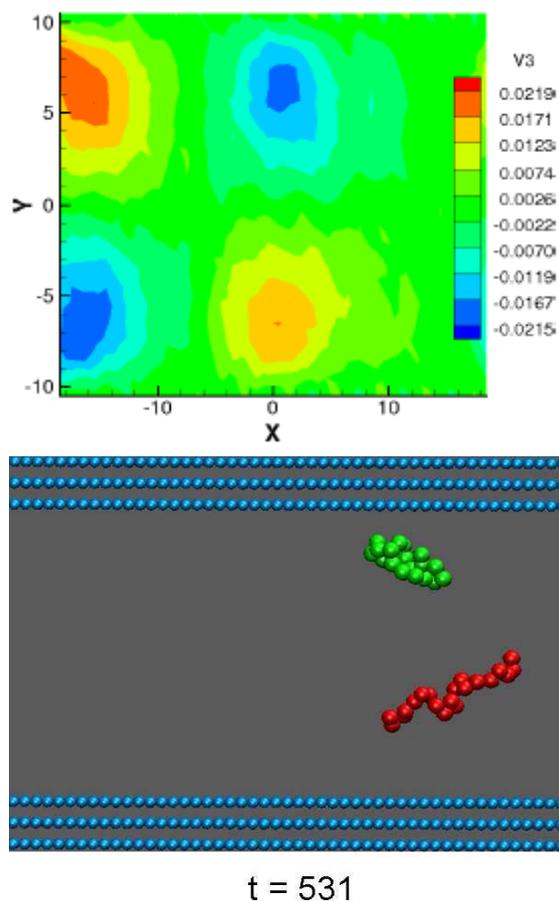
Figure 5: (Top) Contour plot of the transverse velocity profile $u_y(x, y)$ for $kw = \pi/2$, which corresponds to two stripes along the channel length. The blue regions indicate the negative velocity regions and the red regions show the positive velocity regions. The intensity of a color is proportional to the magnitude of the transverse velocity. (Bottom) A snap-shot of chain conformations in the center of the channel and near the wall. Note, the chain in center is more extended compared to the chain near the wall.

Figure 5 (top) shows the average transverse velocity in the channel for a case where there are two stripes along the channel length (corresponding to $kw = \pi/2$). We have also run simulations for a variety of kw values. Alternate circular regions of high positive and negative transverse velocities were observed in the both upper and lower halves of the x-y-cross section about the channel axis. The transverse velocity is close to zero along the center of the tube and near the walls with a maximum in between. The transverse velocity profiles are anti-symmetric about the center of the channel. Thus if the upper half has a positive transverse velocity region then the lower half has a negative transverse velocity region. This creates fluid flow in the transverse direction in such a way that good mixing is achieved. However, we have observed that these transverse velocity regions do not exactly align with the wall pattern. This observation is consistent with continuum theory which suggests that there is a phase lag of $\pi/2$ between the actual pattern and the transverse velocity response (Hendy *et al*, 2005).

To get a clear picture of what is happening on the molecular level we have taken a snapshot of two polymer chains at different times (Fig. 5, bottom). The polymer molecules are found to change their conformations depending on their position in the channel. In contrast to previous studies (Khare *et al*, 1996) the chains here do not only stretch in the direction of the flow but also appear more compressed when closer to the walls. This might be a direct consequence of using periodic wettable and non-wettable regions. The polymer molecules would like to wet the surface in some regions therefore prefer a more closely bound conformations whereas in the nonwettable regions they would like to get away from the walls and hence take up more elongated conformations. Well developed transverse flows were observed when the radius of gyration of polymers (R_g) is smaller than the pattern length. The average radius of gyration of the polymer chains used in our Poiseuille flow simulations under constant slip boundary condition was $R_g = 5.369\sigma$.

However, in the case of $kw = 2\pi$ the pattern length was 4.8σ which is less than the radius of gyration of the polymers. In this case the transverse flows were suppressed. The ratio of the length of the patterned region to the radius of gyration of polymer chains seems to be an important factor in determining the amount of transverse flow that can be achieved. When the length of a patterned region is comparable with the radius of gyration of the polymer chains then, on average, a polymer chain spans two different wettable wall regions simultaneously. Hence these chains start interacting with the wall as if it is a homogeneous continuum and thus decreasing the transverse flow. In our simulations for $kw = 2\pi$, the length of a patterned region was less than the radius of gyration of polymer chains and we have noticed a significant drop in the transverse velocity. The magnitude of the maximum transverse velocity in this case decreased by a factor of 2 compared to the magnitude of the maximum transverse velocity for $kw = \pi/2$. We have also observed that the transverse flow was not as well developed as in the other cases where R_g was less than the pattern length. This indicates that the length of the patterned regions should be longer than radius of gyration to enhance transverse flows. This is an important result which is not captured by the continuum modelling since it does not contain information about individual chains and hence does not include the length-scale R_g. Simulations with off-set patterning of the walls were also conducted to study their effect on the transverse flow. The off-setting was done by moving the upper wall patterning by 3.2σ to the right and keeping the lower wall's position unchanged. We refer to the earlier case where the patterns were exactly parallel to each other as parallel patterning. Results of the simulations with off-setting in the pattern have shown no significant deviations in the magnitude of the maximum transverse velocity compared to that of parallel patterning. However, the transverse velocity regions in the upper and lower halves of the cross-section do not align parallel to each other as in the case of parallel patterning but they are off-set. This was expected since the off-setting in the patterning leads to different flow behavior on the either side of the channel axis and hence off-setting of transverse flow regions

occurs. An interesting observation from these simulations is that the transverse velocity is non-zero, in certain regions, at the center of the channel. Hence, with this patterning set-up fluid elements in the center of the channel can flow towards the boundaries. In contrast, in the parallel patterning case, the transverse fluid velocity in the center of the channel is always zero and thus these fluid elements would never mix (except through diffusion). Therefore we suggest to obtain good mixing throughout the channel, it is better to have off-set patterned regions on opposite sides of the channel.

Patterned boundaries (time varying pressure)

To simulate a sinusoidal time varying pressure we applied a body force of the form $F = F_0 \left(1 + \varepsilon \sin(\omega t)\right)$ and ran simulations for a number of different angular velocities. When we apply a sinusoidal body force we expect an elastic fluid will also respond with a sinusoidal longitudinal velocity. However, because of viscous dissipation, the fluid will be out of phase with the body force by $\phi \equiv \tan^{-1}(\lambda \omega)$. Indeed this is what we found, indicating our fluid was indeed viscoelastic. However, we did not find a single (unique) relaxation constant but a number of relaxation constants, indicating the simple continuum theory presented above is an adequate starting point but is not entirely correct. Instead we require number of relaxation constants (Bird *et al*, 1987) to fully describe the fluid.

We continued on to carry out simulations with coupled patterned boundaries and time varying pressure gradients. With oscillatory body force, as shown in Fig. 6, the maximum value of the transverse velocity has increased to 0.0288 (compared to a maximum value of 0.0236 in the constant body force case). This represents a 22% increase in the transverse velocity. Results of simulations for other values of ω gave similar increases. In general, we find the increase is on average 20%, compared to a constant body force, and given we have applied a maximum 10% increase in the body force this represents a reasonable increase. We see that the maximum transverse velocity does not change appreciably with increasing frequency. Thus although our simulations agrees with the continuum theory in that a sinusoidally varying body force will increase the transverse velocity, the simulations do not show transverse velocities which increase as ω increases. We believe the reason for this is that the simplified continuum model includes only a single relaxation constant while the fluid modelled is characterised by several relaxation constants. Instead the transverse velocity is a superposition of velocities corresponding to each relaxation constant.

CONCLUSION

In this study we have used both continuum theory and first principle particle simulations to suggest methods to enhance mixing in complex fluids. We have considered a combination of methods, firstly using patterned boundary conditions (with alternating boundary regions of high and low slip) and secondly using a sinusoidally varying pressure gradient. In general both the continuum theory and particle simulations show that using patterned boundary conditions can induce transverse flows in a long channel (which normally would have a simple Pouseille profile). For shear thinning fluids this transverse flow is

smaller than what one would obtain for a Newtonian fluid, but we suggest that coupling the patterned boundaries with a sinusoidally varying pressure gradient can increase the transverse flow significantly.
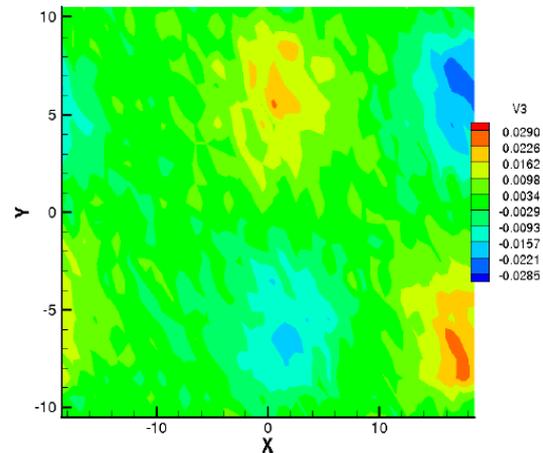
Figure 6: Transverse velocity profile for the time dependent body force case for the frequency $\omega = 2\pi/10$.

REFERENCES

ALLEN, M.P. and TILLDESLEY, D.J., (1987), Computer simulation of liquids, Clarendon Press, Oxford.

BARNES, H.A., HUTTON, J.F., and WALTERS, K., (1989), "An introduction to rheology", Elsevier, Amsterdam.

BIRD, R.B., ARMSTRONG, R.C. and HASSAGER, O., (1987), "Dynamics of polymeric liquids", John Wiley & Sons, New York.

DOI, M and EDWARDS, S.F., (1999) "The theory of polymer dynamics", Clarendon Press, Oxford.

GREST, G.S. and KREMER, K., (1986), "Molecular dynamics simulation for polymers in the presence of a heat bath", *Phys. Rev. A*, **33**, 3628-3631.

HENDY, S.C., JASPERSE, M. and BURNELL, J., (2005), "Effect of patterned slip on micro- and nanofluidic flows", *Phys. Rev. E.,* **72**, 016303-1-8.

JABBARZADEH, A., ATKINSON, J.D., and TANNER, R.I., (2003), "Effects of molecular shape on rheological properties in molecular dynamics simulations of star, H, comb and linear polymer melts", *Macromolecules,* **36**, 5020-5031.

KHARE, R., DE PABLO, J.J. and YETIRAJ, A., (1996), "Rheology of confined polymer melts", *Macromolecules,* **29**, 7910-7918.

NGUYEN, N.T. and WU, Z., (2005), "Interfaced control of pressure driven two-fluid flow in microchannels using electroosmosis", *J. Micromech. Microeng,* **15**, 2289-2297.

OTTINO, J.M. and WIGGINS, S., (2004), "Introduction: mixing in fluids", *Phil. Trans. R. Soc. Lond. A*, **362,** 923-935.

TANNER, R.I., (2002), "Engineering rheology", Oxford Engineering Sciences Series, Oxford